

2022 The 5th International Conference on Renewable Energy and Environment Engineering (REEE 2022), 24–26 August, 2022, Brest, France

In-situ assessment of a solar vacuum tube collectors installation dedicated to hot water production

Julien Gambade^{*}, Hervé Noël, Patrick Glouannec, Anthony Magueresse

Institut de Recherche Dupuy de Lôme, Centre de Recherche Christian Huygens, Rue de Saint-Maudé, 56100 Lorient, France

Received 6 October 2022; accepted 8 October 2022

Available online 25 October 2022

Abstract

In order to improve the contribution of solar thermal energy in moderately insolated regions, solar installations have to be optimized and their heating capacity has to be proven. In this aim, an in-situ thermal performance investigation was carried out on a solar installation of 24 “Water-in-Glass” evacuated tube collectors coupled to their storage unit in a northwest European climate. The aim of the installation is to provide a calf-breeding farm with an intermittent supply of water at 80 °C. The particularity of this solar installation is the specific arrangement of this kind of solar water heater in series and in parallel. Instrumentation was implemented to understand and establish energy balances. An analysis was carried out on four sequences representative of each season. The results show that despite mostly unfavorable sky conditions, the solar installation was capable of providing from 12 to 67% of energy needs for these four sequences.

© 2022 The Author(s). Published by Elsevier Ltd. This is an open access article under the CC BY-NC-ND license (<http://creativecommons.org/licenses/by-nc-nd/4.0/>).

Peer-review under responsibility of the scientific committee of the 5th International Conference on Renewable Energy and Environment Engineering, REEE, 2022.

Keywords: Intermittent solar water heating; Specific arrangement of solar collectors; Water-in-Glass evacuated tubes; In-situ experiment; Operative thermal efficiency; Assessment of thermal performance

1. Introduction

The reduction of energy consumption and the use of low-carbon energies have become a necessity for several years [1]. Solar energy is a widely accessible and renewable energy available all over the world [2]. Solar water heater systems have existed for centuries but there is a need for innovation to improve their performance, particularly in regions with low levels of sunshine. Solar thermal technologies have been developed to maximize the collection and use of solar irradiance [3].

The agricultural sector consumes a significant amount of energy to produce hot water, especially in the northwest Europe region where fossil energies are used for heating water. The development of renewable energy like solar thermal energy is highly recommended to reduce greenhouse gas emissions and to move towards a low-carbon

^{*} Corresponding author.

E-mail address: julien.gambade@univ-ubs.fr (J. Gambade).

<https://doi.org/10.1016/j.egyr.2022.10.160>

2352-4847/© 2022 The Author(s). Published by Elsevier Ltd. This is an open access article under the CC BY-NC-ND license (<http://creativecommons.org/licenses/by-nc-nd/4.0/>).

Peer-review under responsibility of the scientific committee of the 5th International Conference on Renewable Energy and Environment Engineering, REEE, 2022.

Nomenclature

A	Collector gross area (m^2)
cp	Specific heat capacity ($\text{J kg}^{-1} \text{K}^{-1}$)
$H_{D,H}$	Diffuse horizontal irradiation (MJ m^{-2})
$H_{G,H}$	Global horizontal irradiation (MJ m^{-2})
$H_{G,T}$	Global tilted irradiation (MJ m^{-2})
m	mass flow rate (kg h^{-1})
Q_{sup}	Supplied energy (MJ)
Q_{req}	Required energy (MJ)
T_{ave}	Average temperature in tank ($^{\circ}\text{C}$)
T_{top}	Temperature at top of tank ($^{\circ}\text{C}$)
V	Tank volume (m^3)
ρ	Density (kg m^{-3})
η	Efficiency (–)

economy. Solar energy applications in agriculture concern drying processes (crops and grain) and heating water for livestock operations (equipment cleaning and feeding) [4]

Evacuated tube collectors are relevant solutions for hot water production. Each tube is surrounded by a larger glass tube to create a vacuum to minimize thermal losses. Those collectors have a wider operating temperature range and are still more efficient at higher temperatures than flat-plate collectors. The inner tube is covered with an absorbent surface. There are two types of evacuated tubes collectors: ‘water-in-glass’ and ‘heat-pipe’. Heat-pipe evacuated tubes collectors are composed of several tubes associated with a vessel. Each tube contains a copper heat pipe filled with a working fluid. The fluid rises to the header part of the heat-pipe when heated by solar radiation. The heat-pipe header heats the fluid contained in the vessel. Al-Jobbory compared the performances of an Heat-pipe and a Thermosiphon solar water heater [5]. Heat-pipe evacuated tubes collectors supply water at higher temperatures and are efficient under bad weather conditions whereas Thermosiphon systems have better efficiency with no load and intermittent load.

Water-in-Glass evacuated tubes collectors can be combined with an integrated storage. The performance of these systems has been investigated. Morrison et al. assessed the efficiency of this kind of collector [6]. A numerical model was developed to assess the flow rates between the tubes and the storage tank. It was validated experimentally using a Particle Image Velocimetry camera. From their simulations, they showed that the natural circulation flow rate is influenced by solar radiation and the temperature inside the storage tank. A correlation between those two factors and the flow rates was established using Reynolds and modified Rayleigh numbers. Later, Budihardjo and Morrison (2009) implemented the correlation using the Trnsys software to simulate the performance of WIG-ETC over a year in Sidney [7].

The performance of solar water heaters for domestic utilization has been examined. Chow et al. (2011) assessed the energy outputs of WIG-ETC and HP-ETC in a subtropical climate [8]. They found that the HP-ETC has a higher useful annual energy gain. Nevertheless, they obtained approximatively the same payback durations thanks to the lower cost of WIG-ETC.

In order to ensure high water temperatures, collectors have to be hydraulically connected to design the solar collector field. Liu et al. (2012) studied the performance of solar water heaters using the thermosiphon effect arranged in series [9]. They investigated the variation of solar collector efficiency according to their position and the load profiles.

The aim of this publication is to present an in-situ assessment of the thermal performance of a solar field composed of water-in-glass solar water heaters located in France (latitude 48.56 and longitude -2.46). The annual average global horizontal irradiation is 4200 MJ/m^2 and the ambient temperature ranges from 3°C to 22°C . The solar water heaters produce hot water for a calf breeding facility. This kind of application implies intermittent functioning and requires hot water at around 80°C to prepare the herd’s food twice a day.

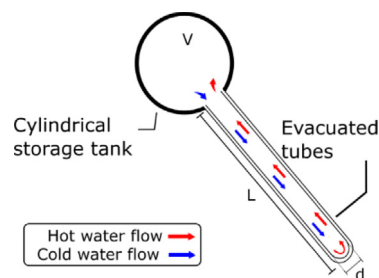
Table 1. Solar collector's parameters.

Tank volume V	241 l
Polyurethane thickness	60 mm
Tubes length L	1,80 m
Inner diameter of tubes d	47 mm
Tubes Volume	79 l

2. Materials and method

2.1. Solar collector

In this study, “Water-in-Glass” collectors are used, they consist of a combination of evacuated tubes and a storage tank (Fig. 1). They are considered as simple and have a low manufacturing cost [10]. Water inside the tubes is heated by solar irradiance. Due to the thermosiphon effect, natural circulation takes place between the evacuated tubes and the water tank. The total volume of the solar water heater is 320 l divided between the storage tank and the evacuated tubes. The water tank is insulated with 60 mm of polyurethane. The collector parameters are given in Fig. 1 and Table 1.

**Fig. 1.** Natural circulation inside the solar collector.

2.2. Solar installation

The use of collectors coupled with stratified tanks enhances the efficiency of the solar conversion. This kind of solar water heater is mostly used individually for domestic applications. The innovative layout of the solar collectors is chosen to optimize the hot water production and the storage in the horizontal cylindrical tank. The solar collector arrangement studied is divided into two parallel rows. Each row contains twelve collectors. The first six solar water heaters are connected in series whereas the last six are in parallel (Fig. 2). The primary function of the in-series collectors is to pre-heat the cold water supplied to the solar installation. The purpose of the parallel collectors is to continue heating the water from the serial collectors as well as to store hot water. The temperature required is 80 °C in order to comply with food preparation recommendations.

The in-series collector tanks are always full whereas the parallel collector tanks can be partially emptied. When hot water is required, a pump is switched on to draw exclusively from the parallel collectors. Installation is supplied with fresh water from the mains water once a minimum level is reached. The hot water contained inside the in-series collectors supplies the partially emptied collectors in parallel. The withdrawals last around 30 to 45 min whereas a filling lasts from 7 to 8 h with a low flow rate (around 5 l/min) to favor thermal stratification inside the storage tanks, thus improving the efficiency of the solar water [11]. Bracamonte et al. (2015) showed that mixing hot water with cold water leads to lower solar water heater efficiency [12]. Pertinent instrumentation was installed to understand and assess the performance of the solar field.

2.3. Instrumentation

The instrumentation was set up on one of the two rows while the facility was already in operation. Consequently, the choice of sensor locations was limited and non-intrusive ultrasonic flowmeters were positioned to measure the inlet and the outlet water flow rates.

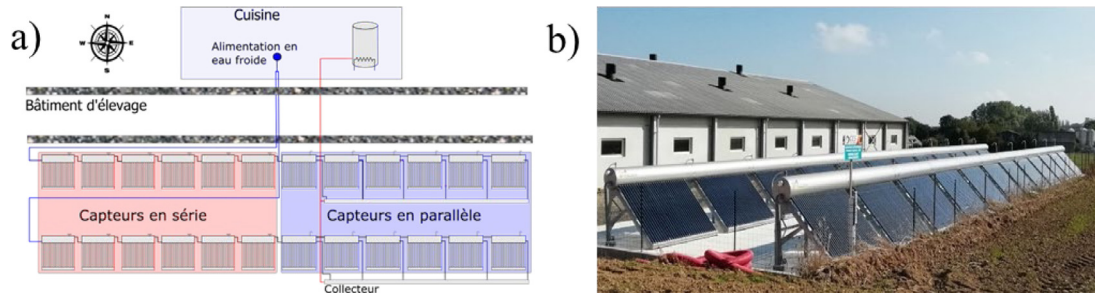


Fig. 2. Scheme (a) and picture (b) of the solar installation.

On-site monitoring of the weather conditions was carried out. A pyranometer measured the global solar radiation received on the horizontal surface and irradiance meters measured the hemispherical irradiance on the front and back of the collector plane. The longwave radiation was determined using a pyrgeometer and allowed calculating the effective sky temperature. The “Thies” weather station gave the wind speed and direction, ambient temperature, relative humidity and atmospheric pressure.

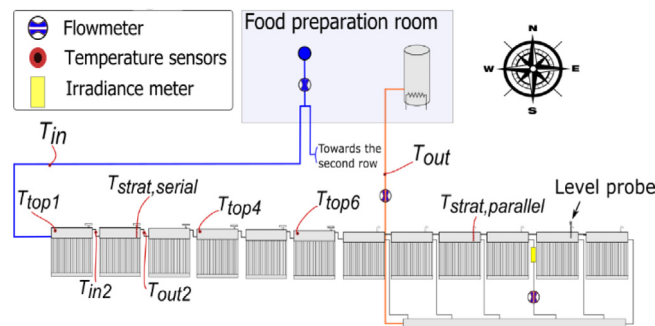


Fig. 3. Instrumentation of the solar installation.

Furthermore, four thermocouples were inserted at the top of the following tanks: the first from the left T_{top1} , the third T_{top3} , the fourth T_{top4} and the sixth T_{top6} . Four temperature sensors were placed inside one serial (no.2) and one parallel collector (no.9) to measure temperatures at different levels of the storage tank. Measurements from those sensors allowed calculating the average temperatures $T_{ave,2}$ and $T_{ave,9}$. Fig. 3 shows a diagram of the experimental setup and the sensor locations. Data were collected online with a one-minute time step acquisition, then averaged over 5 min. The accuracy of the sensors is given in Table 2.

Table 2. Instruments accuracy.

	Flow meter omega FDT 25 W	K-type thermocouple	Pyranometer SPN1	Pyrgeometer IR02	Irradiance meter Si-V-1.5TC-batt
Accuracy	$\pm 5\%$	$\pm 0.2^{\circ}\text{C}$	$\pm 5\%$	$\pm 5\%$	$\pm 5\%$

2.4. Energy balance

The energy supplied during the withdrawal between t_i and t_f is calculated with the following relationship:

$$Q_{sup} = \int_{t_i}^{t_f} \dot{m} \times c_p \times (T_{out} - T_{in}) dt \quad (1)$$

where T_{out} is the manifold outlet temperature, T_{in} the temperature of the town water (i.e. the water temperature that would be provided without the solar installation), \dot{m} is the inlet mass flow rate and c_p is the specific heat capacity.

The energy required is calculated similar to the energy delivered except that the outlet temperature is replaced by the process temperature (80 °C).

$$Q_{req} = \int_{t_i}^{t_f} \dot{m} \times c_p \times (T_{req} - T_{in}) dt \quad (2)$$

A convenient indicator for carrying a performance analysis of the solar installation is the ratio between the energy supplied and the energy required:

$$\text{Coverage ratio} = \frac{Q_{sup}}{Q_{req}} \quad (3)$$

The methodology implemented allowed assessing the energies supplied by the solar installation from the measurements.

3. Results and discussion

3.1. Assessment of energy performance during seasonal experiments

In order to evaluate the thermal performance of the installation for each season over a year, four representative periods of 5 days were selected (Table 3). To carry out a consistent study, the initial times of each period were chosen under steady-state conditions with no irradiance or flowrates.

Table 3. Selected periods.

	Winter	Spring	Summer	Autumn
Dates	14/01/21 to 18/01/21	20/05/21 to 24/05/21	27/08/21 to 31/08/21	27/10/21 to 31/10/21

For each sequence, the weather conditions and the relevant data required to assess energy balances are presented. Then, the calculations described previously are performed and charted.

3.1.1. Winter

Fig. 4 shows the weather conditions during the five days. This is a mainly cloudy sky period with temperatures slightly above 0 °C often encountered on site in winter.

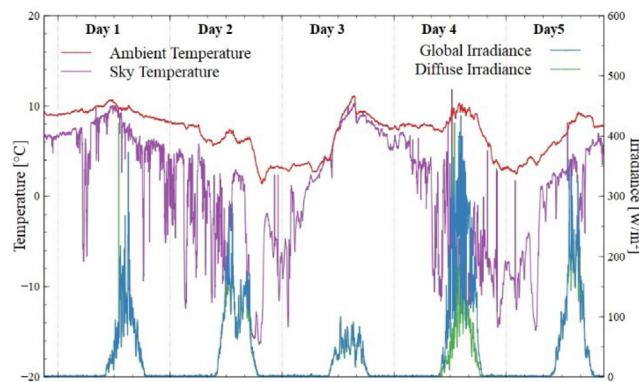


Fig. 4. Winter weather conditions.

The progressive heating along the row can be seen in Fig. 5. T_{top2} and T_{top9} are the temperatures measured by the immersed sensors located at the top of collectors 2 and 9 (Fig. 3). Collector 9 is that of the in-parallel collectors designed to store heated water and to increase the temperature of the latter until withdrawal to the heater vessel.

Fig. 5 shows the inlet and outlet temperatures of the instrumented row during withdrawal. The average temperature of the town water is 6 °C whereas the outlet temperature varies from 11 °C to 28 °C. It is lower than the required temperature but still contributes to reducing fossil energy consumption.

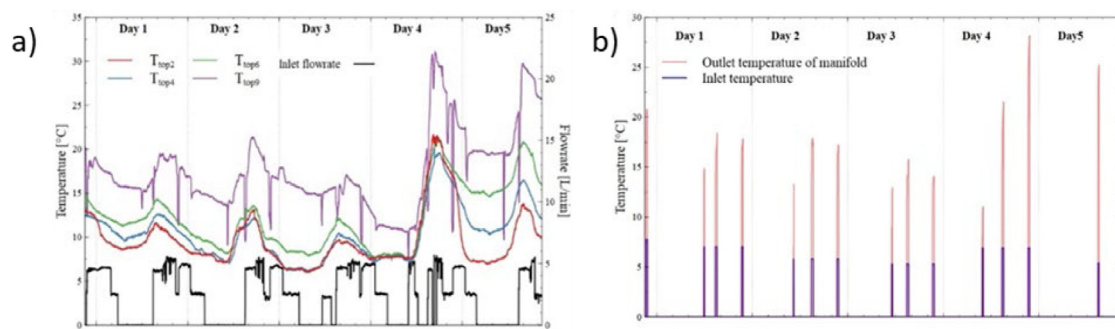


Fig. 5. (a) Temperature at top of tanks (winter) and (b) Inlet and outlet temperatures of a row (winter).

3.1.2. Spring

During this sequence the average ambient temperature is around 12 °C and the sky is partially cloudy (Fig. 6). The reflection of solar irradiance on the surrounding scattered clouds is added to the direct beam. Therefore, the measured global irradiance is occasionally higher than the expected value in clear sky conditions (930 W/m²).

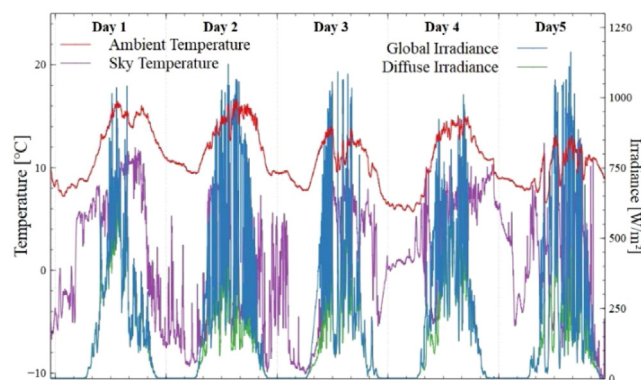


Fig. 6. Spring weather conditions.

For this period, the breeding cycle is nearing completion so required hot water volumes are more substantial, which implies longer filling durations. The progressive increase in temperature in the in-series collectors is particularly obvious in these favorable conditions (Fig. 7). The in-parallel collector temperature peaks every day at around 80 °C. After each withdrawal, this collector is refilled with water from the last in-series collector. Once full, i.e. when the inlet flow rate is null, the temperature in the collector tank is always above 40 °C. The shape of the temperature curves is the same as that observed for the winter period. Fig. 7 presents the temperature difference between the town water and the outlet of the manifold collecting the in-parallel tanks water at each withdrawal. During this experimental sequence, the average outlet temperature is close to 60 °C whereas the inlet temperature is around 11 °C. The solar installation provides a significant part of the energy needs in this period of heavy demand and despite cloudy sky conditions.

3.1.3. Summer

In the course of this summer sequence, the three first days are cloudy and the two following days are almost totally overcast as can be seen through the identical values of global and diffuse irradiances (Fig. 8). The ambient temperature hardly exceeds 20 °C whereas the sky temperature fluctuates between 0 °C during clear sky periods and close to the outdoor temperature in overcast ones.

As a new breeding cycle has recently begun, water needs are not considerable, as can be seen through the inlet flow durations in Fig. 9. The progressive temperature increase in the in-series connected collectors is particularly obvious during night-time. All along the first three days, apart from collector no. 2, the internal energy of the tanks

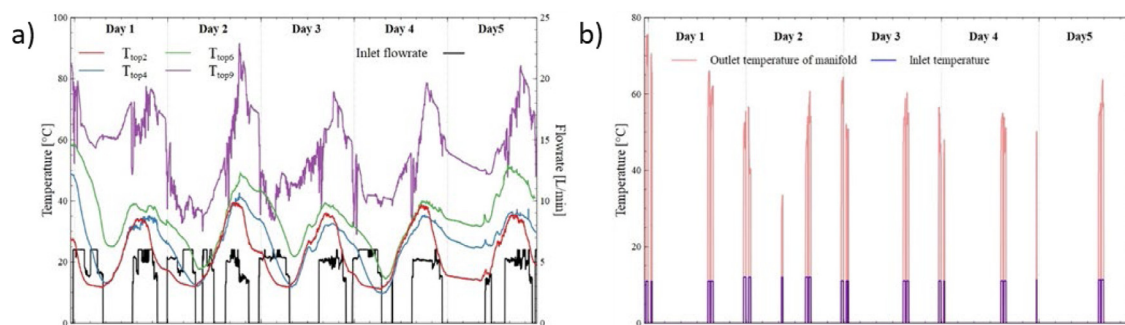


Fig. 7. (a) Temperature at top of tanks and (b) Inlet and outlet temperatures of a row (spring).

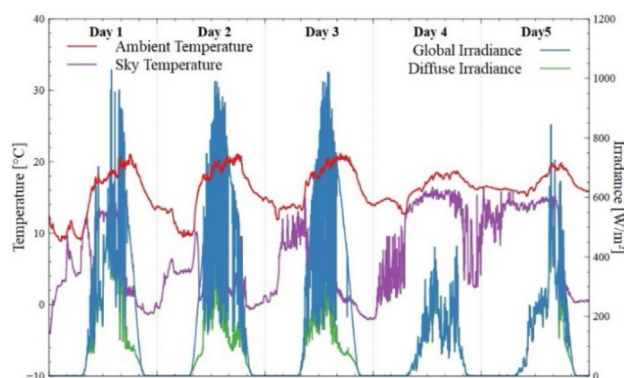


Fig. 8. Summer weather conditions.

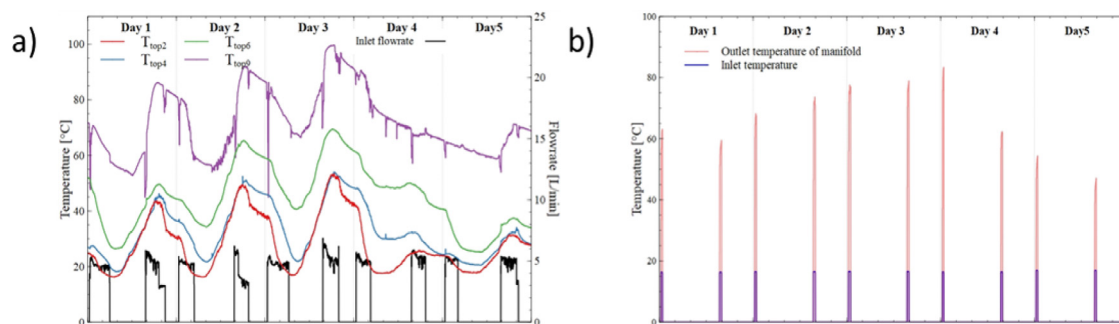


Fig. 9. (a) Temperature at top of tanks and (b) Inlet and outlet temperatures of a row (summer).

increases and then decreases during the overcast days. As the amount of fresh water is moderate, not all the in-series collectors have to be filled with cold water, thus constituting a reserve for the next withdrawals.

The third day, the temperature in the top part of the tank of the ninth collector reaches 100 °C due to the energy stored previously and a rather sunny day. On this day, the water leaving the manifold, a mix of the water coming from the tank of the in-parallel collectors, is above 80 °C, the temperature required to prepare the calves' food (Fig. 9). Thereafter, this temperature remains over 50 °C despite two days with mainly diffuse irradiance.

3.1.4. Autumn

The irradiances and the sky temperature curves reveal the cloudy nature of the sky all along this sequence (Fig. 10). The air temperature evolves between 10 and 17 °C whereas the sky temperature decreases to −8 °C in the rare cloudless periods.

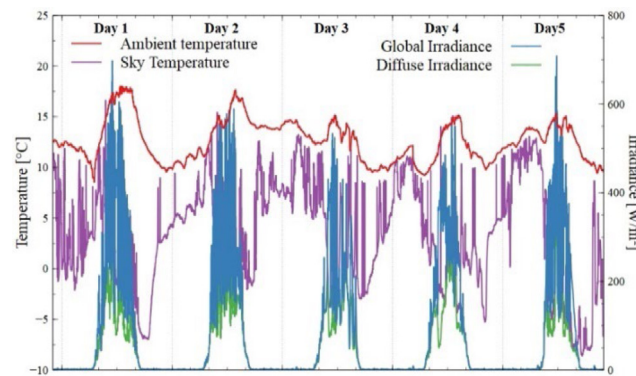


Fig. 10. Autumn weather conditions.

The frequency and duration of the inlet flow rate proves that at this breeding period a very large quantity of water is required to prepare the calves' food (Fig. 11). The energy stored initially is quite high, as after being filled and before dawn the in-parallel collector tank temperature is close to 35 °C. In the course of the two first days, poor irradiance combined with additional water consumption leads to the convergence of in-series tanks temperatures, which means the stored energy is running out. Thereafter, a moderate water consumption gives the installation the opportunity to recover energy despite cloudy conditions.

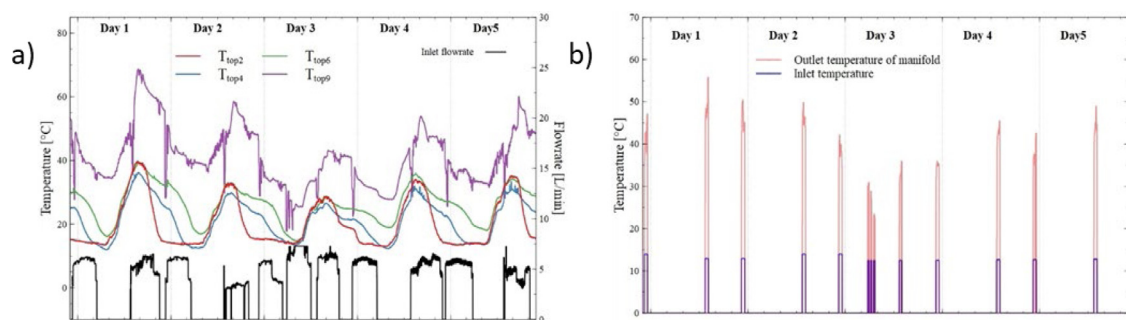


Fig. 11. (a) Temperature at top of tanks and (b) Inlet and outlet temperatures of a row (autumn).

Throughout the experimental sequence, except for the third day when water needs were unusual, the manifold outlet temperature is above 40 °C whereas the town water temperature is lower than 15 °C (Fig. 11).

3.2. Energy considerations

For each sequence studied, Table 4 gives the different irradiations received by the solar installation. Irradiance is mostly diffuse during the four sequences, particularly in winter when the share of diffuse irradiance represents 76% of the solar flux.

The irradiations are calculated from measurements performed in the same way as mentioned previously. $H_{G,H}$ and $H_{D,H}$ are determined from the global horizontal and the diffuse horizontal irradiances given by the SPN1 sensor. The tilted (45°) irradiation is determined using data collected from the irradiance meter located in the plane of the collectors.

The 45° tilt of the solar collector improves the incident irradiation in winter and autumn when the irradiation is lower. In winter, the difference is not as clear due to a very cloudy sequence with very few direct irradiances, as highlighted by the high $H_{D,H}/H_{G,H}$ ratio. In clear sky conditions this ratio should be within 20% at the end of spring and 30% at the end of the year. The best sequence, from this point of view, is the autumn one, for which this ratio is 50%, i.e. around twice the value of a clear sky period at this season. On the contrary, this tilt is disadvantageous more particularly in spring where the noon sun elevation is higher. Nevertheless, in the case of annual operation,

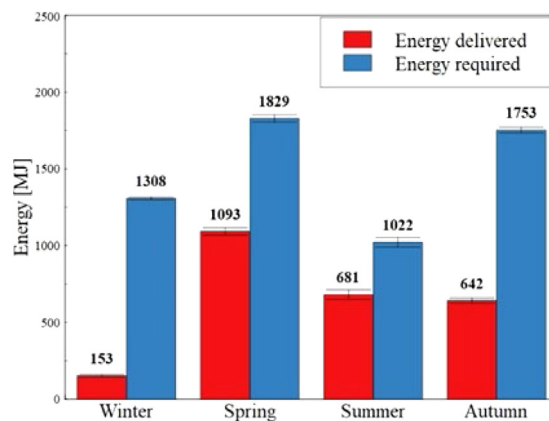
Table 4. Irradiations measured for each period.

	Winter	Spring	Summer	Autumn
$H_{G,H}$ (MJ/m ²)	15.9 ± 1.6	88.9 ± 8.9	70.6 ± 7.1	37.8 ± 3.8
$H_{G,T}$ (MJ/m ²)	21.2 ± 2.1	74.6 ± 7.5	66.8 ± 6.7	62.0 ± 6.2
$H_{D,H}$ (MJ/m ²)	12.1 ± 1.2	53.6 ± 5.4	38.1 ± 3.8	19.4 ± 1.9

tilting the evacuated tubes is highly recommended. The tilted angle can be optimized depending on the latitude of the site and seasonal needs.

The bar chart in Fig. 12 compares, for each experimental sequence, the amount of energy required by the process to the energy provided by the solar installation. In spring and autumn, the calves are in the final part of their breeding and the town temperatures are of the same magnitude thus leading to almost identical required energies. In the winter and summer sequences, as the calves are young they do not need as much food, therefore the energy required is significantly less substantial. The difference between winter and summer lies in the more than 10 °C gap between town water temperatures.

The energy provided by the solar installation (Q_{sup}) is calculated according to Eq. (1) and plotted in Fig. 12. It strongly depends on the weather conditions, mainly the global irradiance and the ambient temperature. Thus, poor weather conditions combined with a moderate amount of water lead to a weak delivered energy. On the contrary, the spring sequence with a large water input and much more favorable weather conditions is the most productive period. The energy delivered by the solar installation in the summer and fall experiments are similar but not for the same reasons. In autumn, the volume of water is large and the temperature level intermediate whereas in summer the volume of water heated is smaller but at a higher temperature. Therefore, the coverage ratio of energy supplied to the energy required (Eq. (4)) is higher in summer (67% in summer and 37% in autumn). In the spring period, while the needs are similar to those of autumn, the coverage ratio reaches 60% due to more favorable irradiations (Table 4). By contrast, the ratio in winter is low (12%) due to very poor weather conditions.

**Fig. 12.** Energy balance of one row.

The energy calculations carried out up to this point do not consider the internal energy variations of the tanks as there was no sensor inside each collector. This energy is far from negligible, particularly if a short time sequence is considered. Nevertheless, this variation may be neglected if the initial and final water tank temperatures differ slightly as in the autumn sequence. It is therefore possible to estimate the overall efficiency of the solar installation for this period. This calculation is done using the global horizontal irradiation and the global tilted irradiation with the following equations:

$$\eta_{O,H} = \frac{Q_{sup}}{H_{G,H}} \text{ and } \eta_{O,T} = \frac{Q_{sup}}{H_{G,T}} \quad (4)$$

In these conditions, the overall efficiencies are equal to 35% and 22% respectively.

4. Conclusion

In this study, an in-situ thermal performance investigation was carried out on a solar installation of 24 “Water-in-Glass” evacuated tube collectors intended to provide hot water to a breeding facility. In order to prepare the herd’s food, a large amount of water at 80 °C is required. Therefore, the vacuum tube collectors coupled with a storage vessel and their specific arrangement were designed to optimize batch withdrawals twice a day.

After having described the solar collector chosen, the actual solar installation located in western France was described. The instrumentation set up in the framework of this study and the method used to acquire the data used to perform energy calculations were presented.

Energy calculations were carried out on four experimental sequences representative of the four seasons. For each of them, weather conditions, running observations and energy calculations were provided. The northwest European climate has a poor solar energy potential and as shown by the high fraction of diffuse irradiation, none of the sequences was especially favorable for a solar installation. Nevertheless, it delivered at least 12% of energy needs during the winter period with very bad weather conditions. The contribution increases to 67% in summer when the conjunction of moderate water consumption and higher solar irradiation made it possible to cover 100% of these needs for some withdrawals.

This study highlighted the capacity of this specific installation composed of “Water-in-Glass evacuated tubes” coupled with a storage unit to contribute supplying high temperature water. This unconventional arrangement along with the specific operating parameters lead to an overall solar conversion efficiency of 35% in a cloudy autumn sequence. Such solar installation, even in regions with moderate insolation, can drastically help mitigating fossil energy consumption. There are ways to improve the performance of the specific arrangements of solar water heaters. The process can be optimized by withdrawing hot water at different time and another ratio of series to parallel collectors could be studied.

Declaration of competing interest

The authors declare that they have no known competing financial interests or personal relationships that could have appeared to influence the work reported in this paper.

Data availability

Data will be made available on request.

Acknowledgments

This research was carried out in the framework of the ICare4Farms project, funded by the INTERREG North West Europe program, France. Fengtech designed the solar installation and made it available for instrumentation.

References

- [1] Letcher TM. Global warming—a complex situation. In: *Climate change*. Elsevier; 2021, p. 3–17. <http://dx.doi.org/10.1016/B978-0-12-821575-3.00001-3>.
- [2] Právělie R, Patriche C, Bandoc G. Spatial assessment of solar energy potential at global scale. A geographical approach. *J Clean Prod* 2019;209:692–721. <http://dx.doi.org/10.1016/j.jclepro.2018.10.239>.
- [3] Sabiha MA, Saidur R, Mekhilef S, Mahian O. Progress and latest developments of evacuated tube solar collectors. *Renew Sustain Energy Rev* 2015;51:1038–54. <http://dx.doi.org/10.1016/j.rser.2015.07.016>.
- [4] Chel A, Kaushik G. Renewable energy for sustainable agriculture. *Agron Sustain Dev* 2011;31:91–118. <http://dx.doi.org/10.1051/agro/2010029>.
- [5] Al-Joboory HNS. Comparative experimental investigation of two evacuated tube solar water heaters of different configurations for domestic application of Baghdad- Iraq. *Energy Build* 2019;203:109437. <http://dx.doi.org/10.1016/j.enbuild.2019.109437>.
- [6] Morrison GL, Budihardjo I, Behnia M. Measurement and simulation of flow rate in a water-in-glass evacuated tube solar water heater. *Solar Energy* 2005;78:257–67. <http://dx.doi.org/10.1016/j.solener.2004.09.005>.
- [7] Budihardjo I, Morrison GL. Performance of water-in-glass evacuated tube solar water heaters. *Solar Energy* 2009;83:49–56. <http://dx.doi.org/10.1016/j.solener.2008.06.010>.
- [8] Chow T-T, Dong Z, Chan L-S, Fong K-F, Bai Y. Performance evaluation of evacuated tube solar domestic hot water systems in Hong Kong. *Energy Build* 2011;43:3467–74. <http://dx.doi.org/10.1016/j.enbuild.2011.09.009>.
- [9] Li Z, Chen C, Luo H, Zhang Y, Xue Y. All-glass vacuum tube collector heat transfer model used in forced-circulation solar water heating system. *Solar Energy* 2010;84:1413–21. <http://dx.doi.org/10.1016/j.solener.2010.05.001>.

- [10] Morrison GL, Budihardjo I, Behnia M. Water-in-glass evacuated tube solar water heaters. *Solar Energy* 2004;76:135–40. <http://dx.doi.org/10.1016/j.solener.2003.07.024>.
- [11] Assari MR, Basirat Tabrizi H, Savadkohy M. Numerical and experimental study of inlet-outlet locations effect in horizontal storage tank of solar water heater. *Sustain Energy Technol Assess* 2018;25:181–90. <http://dx.doi.org/10.1016/j.seta.2017.12.009>.
- [12] Bracamonte J, Parada J, Dimas J, Baritto M. Effect of the collector tilt angle on thermal efficiency and stratification of passive water in glass evacuated tube solar water heater. *Appl Energy* 2015;155:648–59. <http://dx.doi.org/10.1016/j.apenergy.2015.06.008>.